Invariance of the Solid–Liquid Interfacial Energy in Electrowetting Probed via Capillary Condensation

ARTICLE *in* LANGMUIR · JULY 2010

Impact Factor: 4.46 · DOI: 10.1021/la101255t · Source: PubMed

3 AUTHORS:

Rohini Gupta
University of Pennsylvania
7 PUBLICATIONS **59** CITATIONS
SEE PROFILE

Gloria K. Olivier
University of California, Berkeley
12 PUBLICATIONS **138** CITATIONS
SEE PROFILE

Joelle Frechette
Johns Hopkins University
40 PUBLICATIONS **418** CITATIONS
SEE PROFILE

Langmuir
Article
pubs.acs.org/Langmuir

Invariance of the Solid−Liquid Interfacial Energy in Electrowetting Probed via Capillary Condensation

Rohini Gupta, Gloria K. Olivier, and Joelle Frechette*

Department of Chemical and Biomolecular Engineering, Johns Hopkins University, Baltimore, Maryland 21218

Received March 30, 2010. Revised Manuscript Received May 19, 2010

Capillary condensation is employed to probe the solid−liquid interfacial energy in electrowetting on dielectric. The height of an annular water meniscus formed via capillary condensation inside the surface force apparatus is measured as a function of the potential applied across the meniscus and the dielectric stack where the meniscus is formed. According to the Kelvin equation, a decrease in the solid−liquid interfacial energy at constant temperature and relative humidity should lead to an increase in the meniscus height. Our experimental results on nanometer-sized meniscus are in agreement with the work of Mugele [*J. Phys.: Condens. Matter* **2007**, *19*, 375112] and unequivocally demonstrate that the real contact angle (or the solid−liquid interfacial energy) remains unaltered in electrowetting on dielectric.

Introduction

Electrowetting on dielectric (EWOD) is an effective method to direct fluids on a surface[1−3] and has been successfully employed in digital microfluidics,[4,5] optical applications such as autofocus lenses,[6,7] and display systems.[8,9] While being a promising technology, the mechanism at play during electrowetting is not fully understood and the nature of anomalous features such as contact angle saturation remains debated. Two approaches originating from different mechanisms (electrocapillarity and electromechanics) have been proposed to describe the observed change in apparent contact angle of a drop with applied potential in electrowetting.[1] Interestingly, these different theories lead to the same macroscopic response (i.e., the relationship between apparent contact angle and voltage is the same). Therefore, it has been difficult to unequivocally explain the underlying physics based on sessile drop measurements. Recent calculations and experimental results strongly favor the electromechanical arguments. The electrocapillary formalism, however, is still widely used in the literature[10−18] and has been employed to explain contact angle saturation.[19,20] Without the ability to monitor the real contact angle at the triple contact line (TCL), it is difficult to rule out some contribution from electrocapillarity in electrowetting. Additional experimental evidence, especially looking directly at changes of the solid−liquid interfacial energy could help resolve this issue.

Using classical thermodynamics, Lippmann[21] predicted a change in electrode−electrolyte interfacial energy under the influence of an applied potential due to the rearrangement of the double layer at the interface (electrocapillarity). The electrocapillary approach[1] has been widely used to describe the change in contact angle with an applied potential in electrowetting until the recent work of Mugele[22−24] and Jones[25] highlighted its shortcomings. The electrocapillary view predicts that the contact angle change in response to the applied potential ($\theta(V)$) follows the Young-Lippmann or electrowetting equation (eq 1) on a length scale at which the entire dielectric stack (including the electrical double layer) can be treated as a part of the "effective" interface and the free energy change of the dielectric due to polarization can thus be assumed to alter the solid−liquid interfacial energy. The electrocapillary formalism thus implies that the contact angle follows eq 1 up to the TCL.

$$\cos\theta = \cos\theta_o + \frac{cV^2}{2\gamma_{LV}} \tag{1}$$

In eq 1, θ_o is the initial contact angle, c is the capacitance per unit area of the dielectric stack, V is the applied potential, and γ_{LV} is the liquid−vapor interfacial energy.

The electromechanical approach, on the other hand, states that the spreading of a conductive drop on a dielectric in response to the applied potential is due to fringe fields near the TCL resulting from the nonuniform charge distribution and associated Maxwell stress. Near the TCL, this Maxwell stress diverges and leads to a

*Corresponding author. Telephone: (410) 516-0113. Fax: (410) 516-5510. E-mail: jfrechette@jhu.edu.

(1) Mugele, F.; Baret, J. C. *J. Phys.: Condens. Matter* **2005**, *17*, R705–R774.
(2) Gras, S. L.; Mahmud, T.; Rosengarten, G.; Mitchell, A.; Kalantar-Zadeh, K. *Chemphyschem* **2007**, *8*, 2036–2050.
(3) Shamai, R.; Andelman, D.; Berge, B.; Hayes, R. *Soft Matter* **2008**, *4*, 38–45.
(4) Pollack, M. G.; Fair, R. B.; Shenderov, A. D. *Appl. Phys. Lett.* **2000**, *77*, 1725–1726.
(5) Squires, T. M.; Quake, S. R. *Rev. Mod. Phys.* **2005**, *77*, 977–1026.
(6) Berge, B.; Peseux, J. *Eur. Phys. J. E* **2000**, *3*, 159–163.
(7) Kuiper, S.; Hendriks, B. H. W. *Appl. Phys. Lett.* **2004**, *85*, 1128–1130.
(8) Hayes, R. A.; Feenstra, B. J. *Nature* **2003**, *425*, 383–385.
(9) Zhou, K.; Heikenfeld, J.; Dean, K. A.; Howard, E. M.; Johnson, M. R. *J. Micromech. Microeng.* **2009**, *19*, 065029_1–12.
(10) Quinn, A.; Sedev, R.; Ralston, J. *J. Phys. Chem. B* **2003**, *107*, 1163–1169.
(11) Berry, S.; Kedzierski, J.; Abedian, B. *J. Colloid Interface Sci.* **2006**, *303*, 517–524.
(12) Millefiorini, S.; Tkaczyk, A. H.; Sedev, R.; Efthimiadis, J.; Ralston, J. *J. Am. Chem. Soc.* **2006**, *128*, 3098–3101.
(13) Berry, S.; Kedzierski, J.; Abedian, B. *Langmuir* **2007**, *23*, 12429–12435.
(14) Wang, Z.; Ou, Y.; Lu, T. M.; Koratkar, N. *J. Phys. Chem. B* **2007**, *111*, 4296–4299.
(15) Bhushan, B.; Ling, X. *J. Phys.: Condens. Matter* **2008**, *20*, 485009_1–10.
(16) Guan, L.; Qi, G. C.; Liu, S.; Zhang, H.; Zhang, Z.; Yang, Y. L.; Wang, C. *J. Phys. Chem. C* **2009**, *113*, 661–665.
(17) Roques-Carmes, T.; Gigante, A.; Commenge, J. M.; Corbel, S. *Langmuir* **2009**, *25*, 12771–12779.
(18) Wang, Y. L.; Bhushan, B. *Langmuir* **2010**, *26*, 4013–4017.
(19) Quinn, A.; Sedev, R.; Ralston, J. *J. Phys. Chem. B* **2005**, *109*, 6268–6275.
(20) Kedzierski, J.; Berry, S. *Langmuir* **2006**, *22*, 5690–5696.
(21) Lippmann, G. *Ann. Chim. Phys.* **1875**, *5*, 494–549.
(22) Buehrle, J.; Herminghaus, S.; Mugele, F. *Phys. Rev. Lett.* **2003**, *91*, 86101_1–4.
(23) Bienia, M.; Vallade, M.; Quilliet, C.; Mugele, F. *Europhys. Lett.* **2006**, *74*, 103–109.
(24) Mugele, F.; Buehrle, J. *J. Phys.: Condens. Matter* **2007**, *19*, 375112_1–20.
(25) Jones, T. B. *J. Micromech. Microeng.* **2005**, *15*, 1184–1187.

nonuniform drop curvature (Laplace pressure). A force balance including the horizontal component of this electrostatic force integrated over the entire drop (while keeping the solid−liquid interfacial energy constant) is sufficient to describe the observed change in apparent (macroscopic) contact angle. At the TCL, this electrostatic force is zero. Therefore, the real (microscopic) contact angle remains constant and equal to the value determined by Young's equation under no applied potential. Thus, far from the solid−liquid interface, the drop remains a spherical cap whose apparent contact angle is described the electrowetting equation (eq 1) while near the TCL, the curvature diverges and the real contact angle remains unaltered even as the applied potential changes.[1,22−24,26]

Evidence pointing toward the electromechanical view include numerical and experimental work of Mugele,[22−24] along with the arguments proposed by Jones.[25] Using numerical methods to simultaneously calculate the electric field and the drop surface profile, Mugele predicted that due to the field induced curvature, the real and apparent contact angle are quite different in electrowetting.[22,23]Jones reasoned that the capillary height-of-rise of a conducting liquid (such as water) in a vertical column formed between two dielectric-coated electrodes is governed by the electromechanical force that arises due to the nonuniform charge distribution close to TCL and thus, is independent of the meniscus curvature and the liquid−dielectric interfacial energy.[25] Experimentally, it is difficult to distinguish between the two underlying mechanisms because far away from the solid−liquid interface, both approaches predict the same change in the apparent contact angle with applied potential. Mugele[24] observed a nonuniform curvature near the TCL, along with a different real contact angle near the solid−liquid interface compared to the angle obtained from the macroscopic drop shape. Their raw images are conclusive evidence that the electromechanical approach overrides electrocapillary approach as it can explain the drop shape both near (qualitatively) and away (quantitatively) from the interface. However, limitations in the optical resolution of the imaging techniques used to monitor changes close to the TCL and possible effects due to contact angle hysteresis make it hard to ascertain whether or not there is any change in the solid−liquid interfacial energy in electrowetting.

In this paper, we present experimental results that unequivocally demonstrate that the solid−liquid interfacial energy remains unaltered in electrowetting and that the mechanism at play is, therefore, electromechanical in nature. Our capillary condensation experiments allow us to probe contact angle changes within the first tens of nanometers of the solid−liquid interface and are not subject to possible issues caused by contact angle hysteresis.

Background

Capillary condensation is a barrier-less nucleation of undersaturated vapors in a nanopore that is favored by negative (concave) curvature of the meniscus. This phenomenon is described by the Kelvin equation (eq 2), which has been verified experimentally for curvature as low as 4 nm.[27,28]

$$\frac{R_g T}{v_L} \ln\left(\frac{P}{P_{sat}}\right) = 2H\gamma_{LV} \qquad (2)$$

In eq 2, R_g is the gas constant, P/P_{sat} is the partial pressure of the vapors, H is the mean curvature of meniscus, v_L is the molar volume of the fluid, and γ_{LV} is the vapor−liquid interfacial energy at a temperature T.

The ability of the surface force apparatus (SFA)[29,30] to independently measure the surface separation and refractive index using multiple beam interferometry (MBI)[31] makes it an ideal tool to investigate the formation of liquid meniscus between surfaces (such as in capillary condensation).[27,32] In MBI, interference due to transparent material between reflecting layers on the two surfaces leads to transmission at specific wavelengths. The shape and wavelengths of interference fringes in a spectrograph reflect the geometry of interaction and are used to determine the refractive index of the material and the separation between the surfaces with a resolution of 0.1−0.3 nm.[29,30,33] The meniscus appears as a discontinuity in the fringes of equal chromatic order.[32] The separation between the two surfaces at this discontinuity is used to extract the meniscus height. The SFA can also be adapted to study of electrical effects.[34−38] The ability to externally control the charging of the surfaces in the SFA was exploited here to look for a possible contribution from electrocapillarity in electrowetting of a liquid meniscus bridging between two surfaces.

Experimental Details

Surface Preparation. Muscovite mica pieces (Ruby, ASTM V-1, S&J Trading) were cleaved in a laminar hood and placed on a larger clean mica backing sheet. The cleaved mica pieces (thickness $=2-4\ \mu$m, $\varepsilon_r = 6-7$[39]) were coated with 50 nm of silver (99.999% purity, Alfa Aesar) via thermal evaporation (Kurt J. Lesker Nano38) at a rate of 3−4 Å/s. The back-silvered mica pieces were glued (Epon 1004 epoxy) onto cylindrical supports (radius of curvature, $R \approx 1-2$ cm). On the alternate side of the silvered mica pieces, 500 nm thick layer of Cytop (CTL-809M, Asahi Co., $\varepsilon_r = 2.1$) was spin coated, followed by annealing at 180 °C for 15 min under vacuum to generate a hydrophobic dielectric stack having a contact angle of 110° with water. The Cytop-coated surface thus obtained had a low contact angle hysteresis (8−10°) and rms roughness of 0.5 nm as obtained by atomic force microscopy. Prior to spin coating, the mica was immersed for 2 min in 10^{-5} M HCl to neutralize free potassium ions on the cleaved mica surface and treated with water plasma (400 mtorr water vapor and 40 W power) for 10 min to improve mica-Cytop adhesion.

EWOD Measurements. Macroscopic EWOD measurements were performed using a 10 μL deionized water drop, with the potential applied between the silver on the back of the mica-Cytop (ground) and a platinum wire inserted inside the drop. The applied potential was controlled using Burleigh (High voltage DC Op Amp PZ-70) power supply and current was monitored using a Keithley (177 microvolt DMM) ammeter. A goniometer (First Ten Angstroms FTA 125) was used to analyze the drop profile and to estimate the contact angle at each applied voltage.

A circuit analogous to macroscopic EWOD experiments was created inside the SFA, as illustrated in Figure 1. The potential was applied across the dielectric stack with electrical connections made to the silver. The mica−Cytop dielectric stack was connected to the negative terminal of the power supply through the SFA chamber using a two-component conductive epoxy (CW2400,

(26) Mugele, F. *Soft Matter* **2009**, *5*, 3377–3384.
(27) Kohonen, M.; Maeda, N.; Christenson, H. *Phys. Rev. Lett.* **1999**, *82*, 4667–4670.
(28) Kohonen, M.; Christenson, H. *Langmuir* **2000**, *16*, 7285–7288.
(29) Tabor, D.; Winterton, R. H. S. *Proc. R. Soc. London, Ser. A* **1969**, *312*, 435–450.
(30) Israelachvili, J. N. *J. Colloid Interface Sci.* **1973**, *44*, 259–272.
(31) Tolansky, S. *Multiple-Beam Interferometry of surfaces and films*; Oxford University Press: London, 1948.
(32) Maeda, N.; Israelachvili, J. N.; Kohonen, M. M. *Proc. Natl. Acad. Sci. U.S. A.* **2003**, *100*, 803–808.
(33) Israelachvili, J. N.; Adams, G. E. *J. Chem. Soc., Faraday Trans. I* **1978**, *74*, 975–1001.
(34) Frechette, J.; Vanderlick, T. K. *Langmuir* **2001**, *17*, 7620–7627.
(35) Frechette, J.; Vanderlick, T. K. *Langmuir* **2005**, *21*, 985–991.
(36) Frechette, J.; Vanderlick, T. K. *J. Phys. Chem. B* **2005**, *109*, 4007–4013.
(37) Zeng, H.; Tian, Y.; Anderson, T. H.; Tirrell, M.; Israelachvili, J. N. *Langmuir* **2008**, *24*, 1173–1182.
(38) Frechette, J.; Vanderlick, T. K. *Ind. Eng. Chem. Res.* **2009**, *48*, 2315–2319.
(39) Hepburn, D. M.; Kemp, I. J.; Shields, A. J. *IEEE Electr. Insul. Mag.* **2000**, *16*, 19–24.

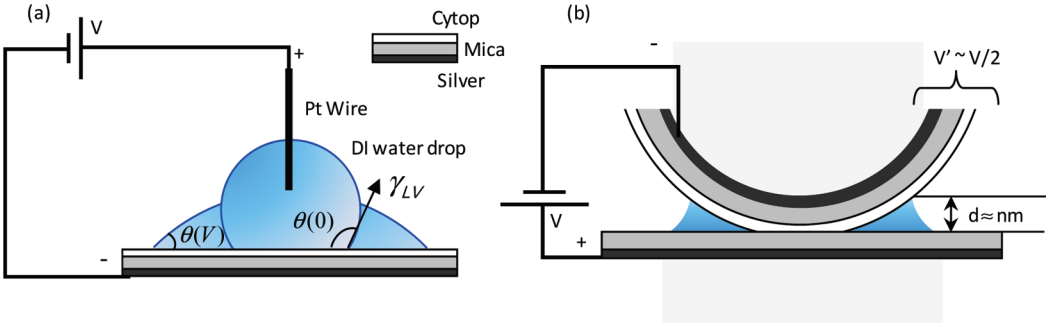

Figure 1. Schematic of the electrical circuit employed (a) for macroscopic EWOD and (b) for capillary condensation inside the SFA. The system configuration inside the SFA mimics macroscopic EWOD.

Chemtronics) such that both the stack and the SFA chamber were grounded. The second surface consisted of back-silvered mica (treated with HCl as mentioned before) and was connected to the positive terminal via a thin flexible shielded wire (AS631, Cooner Wire). Continuity tests were performed throughout the experiments to ensure that the electrical circuit was functional. The change in contact area with applied potential also confirmed that the potential was applied across the surfaces. Negligible current (1−2 nA) was observed throughout the experiments.

Capillary Condensation and SFA. The SFA chamber was thoroughly cleaned and dried with pure nitrogen prior to each experiment. The temperature was monitored throughout the experiment and remained at 25 °C. Undersaturated water vapor were used as the condensable fluid and the relative humidity in the SFA chamber was controlled via supersaturated potassium sulfate solution or pure water, which maintained the relative humidity (RH) at 97% or 98%, respectively. The combination of a hydrophobic and a hydrophilic surface provided us with a meniscus when the surfaces were in contact before any potential was applied. The multimatrix method[40,41] was employed along with a fast spectral correlation algorithm[42] to determine surface separation. The mica thickness was determined by interferometry using pieces having thickness equivalent to those used in the electrowetting experiment. The thickness of the Cytop layer was determined from the fringe positions at contact in the SFA. A CCD camera (Q-Imaging Retiga 4000RV) was used to image the interference fringes obtained inside the spectrograph (Thermo Jarrell Ash).

Results and Discussion

Inside the SFA, when the two surfaces are in contact, the gap between the surfaces outside of the contact region can be viewed as a nanopore. In the presence of condensable vapors, an annular meniscus of fluid (here water) will form as long as the sum of the contact angles of condensing fluid on the two interacting surfaces is less than 180°.[43] Since the cylinder radius is large compared to the meniscus height, the meniscus−vapor interface can be approximated as an arc with a constant radius of curvature, which is known as the circle approximation.[43] The Kelvin equation (eq 2) for the geometry employed here can be expressed in terms of meniscus height, d and the contact angles formed by the fluid with the two surfaces ($\theta_1$and θ_2) and is given by:

$$\frac{R_g T}{v_L}\ln\left(\frac{P_{sat}}{P}\right) = \frac{\gamma_{LV}\{\cos\theta_1 + \cos\theta_2\}}{d} \qquad (3)$$

Thus, at a given partial pressure (relative humidity) and temperature, a change in the real contact angle would cause a condensed meniscus to grow outward to maintain the curvature dictated by the Kelvin equation (eq 3). As this is not a macroscopic phenomenon, only the real contact angle plays a role in the response of the system to the applied field, which makes these experiments well-suited to investigate the role (if any) of electrocapillarity in EWOD. As another added advantage, capillary condensation is not plagued by unwanted effects due to contact angle hysteresis.

If the predictions of the electrocapillary formalism were true for the real contact angle, the meniscus height would increase with the applied potential due a decrease in solid−liquid interfacial energy (or real contact angle). The Young−Lippmann equation can be incorporated into the Kelvin equation (eq 3) to account for a change in the solid−liquid interfacial energy with potential (eq 4). Note that in our experimental configuration, only one surface is hydrophobic (only one of the two surfaces could have its contact angle decreased with potential). Also, the applied potential required for a given change in contact angle in condensation experiments is different than that in a drop experiment because two dielectric layers are present.

$$\frac{R_g T}{v_L}\ln\left(\frac{P_{sat}}{P}\right) = \frac{\gamma_{LV}\left\{\cos\theta_{1,o} + \frac{cV'^2}{2\gamma_{LV}} + \cos\theta_2\right\}}{d} \qquad (4)$$

In eq 4, V' is the voltage across the mica−Cytop stack and the term ($\cos\theta_{1,o} + cV'^2/2\gamma_{LV}$) comes from the Young−Lippmann equation applied to the mica−Cytop stack; $\theta_{1,o}$ is the contact angle of Cytop before any potential is applied and c is the capacitance per unit area of the mica−Cytop stack. The contact angle of mica, θ_2, is ~6−7°[44] and essentially independent of voltage. These experiments are distinct from field induced condensation between an AFM tip and a metal surface driven by the difference in polarizability of air and water.[45,46] In our experimental setup, this contribution is negligible because of the capacitive nature of mica.

Alternatively, the electromechanical approach predicts that the meniscus could spread in response to the electric field due to the nonuniform curvature. However, in the capillary condensation experiments showed here, the field induced local curvature is insignificant (approximately 3 orders of magnitude lower) compared to the mean curvature of the meniscus for the given relative humidity (97% and 98%). Also, for the cases where the local

(40) Clarkson, M. T. *J. Phys. D: Appl. Phys.* **1989**, *22*, 475–482.
(41) Levins, J. M.; Vanderlick, T. K. *Langmuir* **1994**, *10*, 2389–2394.
(42) Heuberger, M. *Rev. Sci. Instrum.* **2001**, *72*, 1700–1707.
(43) Orr, F. M.; Scriven, L. E.; Rivas, A. P. *J. Fluid Mech.* **1975**, *67*, 723–742.
(44) Beaglehole, D.; Radlinska, E. Z.; Ninham, B. W.; Christenson, H. K. *Phys. Rev. Lett.* **1991**, *66*, 2084–2087.
(45) Gómez-Monivas, S.; Sáenz, J. J.; Calleja, M.; García, R. *Phys. Rev. Lett.* **2003**, *91*, 056101_1–4.
(46) Sacha, G.; Verdaguer, A.; Salmeron, M. *J. Phys. Chem. B* **2006**, *110*, 14870–14873.

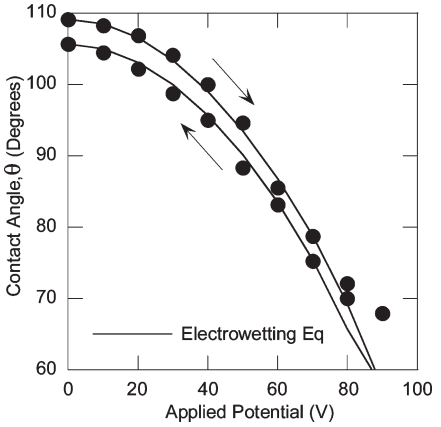

Figure 2. The apparent contact angle of deionized water drop on 2.5 μm mica and 455 nm Cytop in the presence of an applied potential. The solid line represents the electrowetting equation.

fringe fields were to exceed the breakdown strength of the dielectric (mica) in these experiments (which should result in significant current through the electrical circuit), the field induced local curvature would still be negligible. Our experiments are well within this limit, as negligible currents were observed. Therefore, according to electromechanical approach, meniscus height is expected to be mostly independent of applied potential in our experiments.

As a control, we performed macroscopic EWOD experiments on the same mica−Cytop surface using a platinum electrode inserted in a deionized water drop (Figure 2) prior to the condensation experiments. As shown in Figure 2, the surfaces respond to an applied voltage according to the electrowetting equation (eq 1) without any fitted parameters. The electrowetting response is reversible within 2−3° and contact angle saturation is observed at 70°. In addition, to verify the macroscopic electrowetting performance in the SFA configuration (where the meniscus is isolated from the electrode by mica), EWOD measurements were conducted for a macroscopic bridge between the same two surfaces. The variation of apparent contact angle with applied potential in macroscopic bridge configuration follows the electrowetting equation (see Supporting Information).

In the condensation experiments, the height of the meniscus was measured at different applied potentials for both 97% and 98% relative humidity (RH). High relative humidity was chosen to ensure that the meniscus height is readily measurable and that large changes (if any) in the meniscus height are obtained if the solid−liquid interfacial energy changes with the applied potential. The initial meniscus height was used to estimate the relative humidity (97% for 12 nm and 98% for 18 nm at 25 °C) maintained inside the SFA chamber, as per the Kelvin equation. Considering the error of choosing the position of discontinuity, we can resolve the meniscus height with a confidence of ±1.5 nm. Sufficient time was given at each applied potential for the meniscus heights to reach their equilibrium values. This was especially important as the kinetics of capillary condensation can be significant at high relative humidities (Figure 3).[27] We observed that 5−10 min were sufficient for the meniscus to reach its final height at all potentials. Longer wait times, even of the order of 16 h, did not affect the meniscus size at a particular applied voltage.

The meniscus height (normalized with the height at 0 V) as a function of voltage for both 97% and 98% are shown in Figure 4. The dashed/dotted lines corresponding to predictions according to electrocapillarity are plotted for reference. Clearly, the meniscus height variation is insignificant compared to the expectations

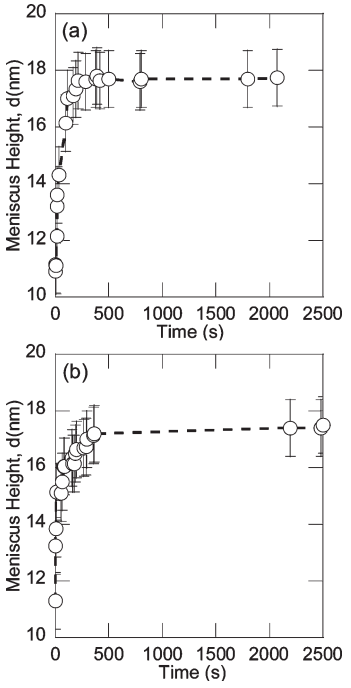

Figure 3. Kinetics of capillary condensation at RH = 98% for applied voltages, (a) 0 V and (b) 150 V. The meniscus reaches its equilibrium height within a few minutes. The dashed lines are drawn to guide the eye.

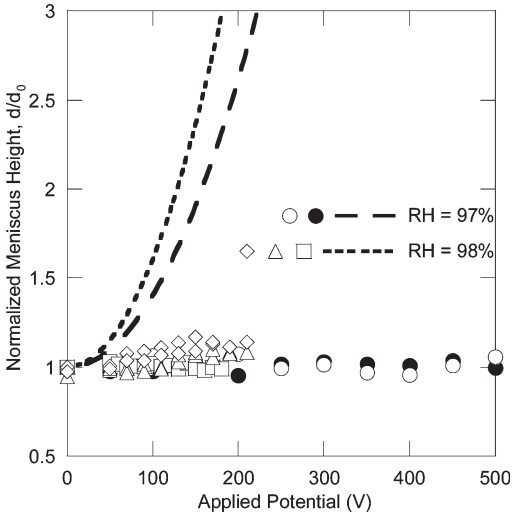

Figure 4. Height of a condensed meniscus (normalized with the height at 0 V) measured as a function of the applied voltage for RH = 97% and 98%. The lines correspond to the theoretical expectations according to the electrocapillary approach.

from the electrocapillary formalism. This implies that there is insignificant contribution from electrocapillarity in electrowetting and, thus the contact angle remains the same as Young's value at all potentials in EWOD. The thermodynamic argument, according to which charging of the double layer is expected to change the solid−liquid interfacial energy in the presence of an electric field, is not applicable for electrowetting on dielectric.[26] The dielectric introduced to circumvent electrolysis limits the potential drop across the double layer such that at all applied potentials, the charge density at the solid−liquid interface is not sufficient to decrease the real contact angle. Thus, the underlying mechanism driving EWOD is not electrocapillarity.

Our results are in agreement with the recent simulations and the experiments of Mugele.[22−24] It is also worth mentioning results from two other experimental studies that agree with the electromechanical nature of electrowetting. Lu et al.[47] studied electrowetting in nanoporous silica and observed a negligible change in solid−liquid interfacial energy in response to applied electric field, unlike what should be expected from electrocapillarity. They attributed this behavior to large surface-volume ratio of liquid confined in the nanopores. However, we believe that their observation is consistent with the electromechanics approach. In another study of nanoscale electrowetting using AFM,[16] variation in the capillary force due to a bridge between a hydrophobic polymer surface and a silicon tip in the presence of an applied field was attributed to changes in solid−liquid interfacial energy. However, this variation in measured capillary force is likely due to the electrostatic force and not a change in the solid−liquid interfacial energy.

Conclusions

Capillary condensation inside the SFA was employed to study changes in the solid−liquid interfacial energy in electrowetting on dielectric. The height of the annular water meniscus formed in a nanopore via capillary condensation inside the SFA was measured as a function of potential applied across the dielectric stack that forms the nanopore. Contact angle change occurring within the first tens of nanometers from the solid−liquid interface formed between nanopore and condensate can be evaluated from the meniscus height. In addition, conducting these experiments in the constant pressure regime ensured that possible issues caused by contact angle hysteresis were avoided. Our experimental results involving condensation convincingly show that the real contact angle is indeed constant in electrowetting on dielectric and enable us to decouple electromechanics from electrocapillarity.

Acknowledgment. This material is based upon work supported by the National Science Foundation under Grant CMMI-0709187, and 3M Corp. Acknowledgment is made to the Donors of the American Chemical Society Petroleum Research Fund for partial support of this research under Grants No. 46510G5. The authors extend their thanks to Jun Ma and Patricia McGuiggan for AFM imaging.

Supporting Information Available: The results from macroscopic electrowetting performed in the same configuration as in the SFA (i.e., macroscopic bridge between two surfaces with the bridge isolated from the electrode by an insulating mica piece). This material is available free of charge via the Internet at http://pubs.acs.org.

(47) Lu, W. Y.; Kim, T.; Han, A. J.; Chen, X.; Qiao, Y. *Langmuir* **2009**, *25*, 9463–9466.